arXiv:1605.02465v1 [physics.plasm-ph] 9 May 2016

Benchmark of a new multi-ion-species collision operator for δf Monte Carlo neoclassical simulation

Shinsuke Satake[a,b,*], Motoki Nataka[a,b], Theerasarn Pianpanit[b], Hideo Sugama[a,b], Masanori Nunami[a,b], Seikichi Matsuoka[c], Seiji Ishiguro[a,b], Ryutaro Kanno[a,b]

[a] *National Institute for Fusion Science, Toki 509-5292, Japan*
[b] *The Graduate University for Advanced Studies, Toki 509-5292, Japan*
[c] *Japan Atomic Energy Agency, Kashiwa 227-0871, Japan*

Abstract

A numerical method to implement a linearized Coulomb collision operator for multi-ion-species neoclassical transport simulation using two-weight δf Monte Carlo method is developed. The conservation properties and the adjointness of the operator in the collisions between two particle species with different temperatures are verified. The linearized operator in a δf Monte Carlo code is benchmarked with other two kinetic simulation codes, i. e., a δf continuum gyrokinetic code with the same linearized collision operator and a full-f PIC code with Nanbu collision operator. The benchmark simulations of the equilibration process of plasma flow and temperature fluctuation among several particle species show very good agreement between δf Monte Carlo code and the other two codes. An error in the H-theorem in the two-weight δf Monte Carlo method is found, which is caused by the weight spreading phenomenon inherent in the two-weight δf method. It is demonstrated that the weight averaging method serves to restoring the H-theorem without causing side effect.

Keywords: Landau collision operator, δf Monte Carlo method, multi-ion-species plasma

*Corresponding author
Email address: satake@nifs.ac.jp (Shinsuke Satake)

1. Introduction

To study and evaluate the neoclassical transport[1, 2, 3] in burning plasmas such as in ITER[4] and future fusion reactors, it is essential to consider the transport process in a plasma containing deuterium, tritium, helium from D-T fusion reaction, and impurity ions such as C, Fe, and W from the vacuum vessel and divertor wall. Neoclassical transport, which is described by drift-kinetic equation for guiding-center distribution function, treats the transport process of the charged ions and electrons in toroidal magnetic field caused by guiding-center drift motion and Coulomb collisions. Therefore, it is required to develop a neoclassical transport simulation code for multi-ion-species plasmas which treats the Coulomb collisions among unlike ion species and electrons. One of the important points in treating the transport process in fusion plasma is that the large differences in the masses of the charged particles. Not only between ions and electrons of which mass ratio is $m_i/m_e > 10^3$, the mass ratio between bulk fuel D or T and heavy impurity ions like W can also be order of 10^2. Because of slow thermal equilibration between two particle species with large mass ratio, and also because of the different energy confinement time scale and different heating rate according to the particle species, it is possible that there remains finite temperature difference among the particle species even in a steady-state long-pulse discharge.

Most of the theories and numerical simulations of neoclassical transport process have been developed by using the linearized Fokker-Planck collision operators, or so called Landau operator, as it is explained in Section 2. The linearized collision operator[5] has important properties for thermodynamics, that is, the adjointness of the operator and the Boltzmann's H-theorem. The former is related to Onsagar symmetry of the neoclassical transport matrix[6], and the latter is understood as the entropy production by collisional process. It describes the dissipative nature of collisions, which damps the distribution function toward a local equilibrium state. Also, in the application of the linearized collision operator in the drift-kinetic equation, it is shown that the entropy production rate coincides with the sum of the inner products of the thermodynamic forces and the conjugate neoclassical fluxes[6]. Therefore, the adjointness and the H-theorem of the linearized operator make the basis of thermodynamics aspects of neoclassical transport theory.

However, it is known that these two properties above are not rigorously satisfied by the Landau operator when the particle species have different tem-

peratures. Therefore, in many of previous studies on the neoclassical transport in multi-ion-species plasmas, it has been usually assumed that all the ion species have the same temperature. Only the temperature difference between ions and electrons are allowed, since the coupling of ions and electrons in the drift-kinetic equation by the collision term is usually unimportant because of its large mass-ratio. As mentioned above, however, two ion particle species with large mass-ratio are also possible to have different temperatures. To investigate the transport process in fusion reactors by numerical simulations, it is required to develop a collision operator for unlike-collisions among the ion species with different temperatures. Recently, Sugama et al *et al.*[7] has invented a modified Landau operator which keeps the adjointness nature even if the temperature of two ion species are different. We plan to extend the neoclassical simulation code FORTEC-3D[8, 9] by implementing the modified linearized Coulomb collision operator for multi-ion-species plasmas. In this paper, a numerical method to implement the collision operator in a δf Monte Carlo particle code like FORTEC-3D is explained. Benchmark of the new collision operator with the same one implemented in a continuum gyrokinetic δf code GKV[10, 11] and the other one in a full-f PIC code based on Nanbu-method[12] are carried out. It will be demonstrated that the linearized operator implemented in the δf Monte Carlo code agrees well with the other two codes and also keeps the conservation and adjointness properties in high accuracy.

The rest of this paper is organized as follows. In Section 2, basic properties of the linearized collision operator is reviewed. The numerical method to implement the Sugama's modified Landau operator to the δf Monte Carlo method is explained in Section 3. Benchmark tests of the collision operator with two different simulation codes are shown in Section 4, where we also discuss about the numerical error appearing in the H-theorem by the weight-spreading effect and the way how to suppress it. Finally the summary is given in Sectoin 5. In the Appendix, the details of the Monte Carlo way to implement the test-particle operator is explained. In this paper, we concentrate on the development of the collisions among ion species, and the numerical problem in the application of the collision operator for electron-ion collisions is also discussed in Section 5 and Appendix.

2. Properties of linearized collision operator

In a δf drift-kinetic simulation code such as FORTEC-3D, the time evolution of a plasma distribution function of a particle species a caused by Coulomb collisions and guiding-center motion in toroidal magnetic field is represented by the following drift-kinetic equation with the linearized Landau operator C_a^L,

$$\frac{\partial \delta f_a}{\partial t} + \dot{\mathbf{Z}} \cdot \frac{\partial}{\partial \mathbf{Z}} \delta f_a = -\dot{\mathbf{Z}} \cdot \frac{\partial}{\partial \mathbf{Z}} f_{Ma} + C_a^L(\delta f_a), \tag{1}$$

where $C_a^L(\delta f_a) = \sum_b \left[C_{ab}^T(\delta f_a) + C_{ab}^F(\delta f_b) \right]$, $\mathbf{Z} = (\mathbf{x}, v_\parallel, v_\perp)$ is the 5-dimensional phase space coordinates, and $\delta f_a(\mathbf{Z}, t) = f_a - f_{Ma}$ represents the perturbation part of the distribution function from the Maxwellian $f_{Ma} = n_a \left(\frac{m_a}{2\pi T_a} \right)^{3/2} \exp\left(-\frac{m_a v^2}{2T_a} \right)$. Note that the summation over the colliding particle species $\sum_b$ includes the self-collision, $b = a$. The nonlinear term $C_{ab}(\delta f_a, \delta f_b)$ is omitted by the ordering assumption $|\delta f / f_{Ma}| \ll 1$. The distribution function is averaged over the fast gyration motion around the magnetic field, so the velocity coordinates are truncated into 2-dimensions, $(v_\parallel, v_\perp)$. Note that throughout this paper, we discuss only on the time evolution of distribution function solely by Coulomb collisions in a uniform plasma. Therefore, instead of Eq. (1), we consider $(d/dt)\delta f_a(\mathbf{v}, t) = C_a^L(\delta f_a)$.

The test- and field-particle operators, C^T and C^F respectively, should satisfy the following properties.

$$\int d^3v C_{ab}^T(\delta f_a) = \int d^3v C_{ab}^F(\delta f_b) = 0, \tag{2}$$

$$m_a \int d^3v \{\mathbf{v}, v^2\} C_{ab}^T(\delta f_a) = -m_b \int d^3v \{\mathbf{v}, v^2\} C_{ba}^F(\delta f_a), \tag{3}$$

$$\int d^3v \frac{\delta f_a}{f_{aM}} C_{ab}^T(\delta g) = \int d^3v \frac{\delta g}{f_{aM}} C_{ab}^T(\delta f_a), \tag{4}$$

$$T_a \int d^3v \frac{\delta f_a}{f_{aM}} C_{ab}^F(\delta f_b) = T_b \int d^3v \frac{\delta f_b}{f_{bM}} C_{ba}^F(\delta f_a), \tag{5}$$

where Eqs. (2) and (3) represents the conservation property of the particle number, momentum, and energy, whereas Eqs. (4) and (5) are the adjointness of the operator. The other important property of Landau operator is Boltzmann's H-theorem,

$$T_a \int d^3v \frac{\delta f_a}{f_{aM}} \left[C_{ab}^T(\delta f_a) + C_{ab}^F(\delta f_b) \right]$$

$$+T_b \int d^3v \frac{\delta f_b}{f_{bM}} \left[C^T_{ba}(\delta f_b) + C^F_{ba}(\delta f_a) \right] \leq 0, \tag{6}$$

where the equality is satisfied if and only if both δf_a and δf_b become shifted Maxwellian,

$$\delta f_a = f_{Ma} \left[\frac{\delta n_a}{n_a} + 2\frac{\delta u_{\parallel a}}{v_a} v_\parallel + \frac{\delta T_a}{T_a} \left(\frac{m_a^2 v^2}{2T_a} - \frac{3}{2} \right) \right], \tag{7}$$

while $\delta u_{\parallel b} = \delta u_{\parallel a}$ and $\delta T_b/T_b = \delta T_a/T_a$ for δf_b. Here, $v_a = \sqrt{T_a/(2m_a)}$ is the thermal velocity. Since we are interested in drift-kinetic equation in which gyro-phase averaged distribution function is considered, only the parallel component of the mean flow, $\delta u_\parallel$, appears in Eq. (7).

It is known that the original linearized Landau operator does not satisfy the properties Eqs. (4)-(6) if $T_a \neq T_b$[5]. Sugama's modified operator, Eq. (31) for C^T_{ab} and Eq. (35) for C^F_{ab} in Ref.[7], is made by modifying Landau operator so that it preserves the adjointness and H-theorem even if $T_a \neq T_b$. The proof is given in the reference paper. It is to be noted that if $T_a \neq T_b$, collisions between two background Maxwellian part $C_{ab}(f_{Ma}, f_{Mb})$ is nonzero, which represents the temperature relaxation process between two particle species. However, the main purpose of neoclassical transport simulation is to evaluate the transport in a plasma with given kinetic profiles $n_a, n_b, T_a, T_b, \cdots$ and we do not usually treat the change in background temperatures, which occurs very slowly in the transport time scale compared to the collisional relaxation of perturbed distribution function to a quasi-steady state. Furthermore, the temperature relaxation process between a light (a) and heavy (b) species occurs in a time scale $(m_a/m_b)(1-T_a/T_b)/\tau_{ab}$, which is much slower than the collisional momentum relaxation time scale, τ_{ab}^{-1}[5]. It means that the large difference $T_a \neq T_b$ is allowed to happen only if the mass ratio of two species are very large, such as between bulk hydrogen and heavy impurity ions, or between ions and electrons. Therefore we ignore here the slow temperature relaxation process on the background Maxwellian in neoclassical transport simulation. Our purpose is to construct a framework of drift-kinetic equation for δf using a linearized collision operator, which ensures the Onsagar symmetry and H-theorem even if $T_a \neq T_b$. Momentum and energy exchange between two particle species occurs only through the δf part of the distribution function in this model.

3. Implementation of Sugama operator in δf Monte Carlo code

Sugama's modified operator has already been implemented and benchmarked in continuum δf gyrokinetic codes[10, 11], where the distribution function is discretized on the velocity space grids $(v_\parallel, v_\perp)$, and the test- and field-particle operators are implemented numerically by finite-difference and numerical integral schemes. On the contrary, the δf Monte Carlo method is a particle code, in which the test-particle operator is represented by the random walk of simulation markers in the velocity space, and the field-particle operator is represented as a source/sink term for the markers' weight. For the like-particle collisions, FORTEC-3D has already implemented such a Monte Carlo way of C_{aa}^T and C_{aa}^F. In this section, we show how the Sugama operator is implemented for unlike-species collisions, $a \neq b$.

The modified test-particle operator is defined as follows:

$$\begin{aligned} C_{ab}^T(\delta f_a) &= C_{ab}^{T0}(\delta f_a) + (\theta_{ab}-1)(\mathcal{P}_a C_{ab}^{T0}\delta f_a + C_{ab}^{T0}\mathcal{P}_a \delta f_a) \\ &\quad +(\theta_{ab}-1)^2 \mathcal{P}_a C_{ab}^{T0}\mathcal{P}_a \delta f_a, \qquad (8) \\ \theta_{ab} &\equiv \sqrt{T_a\left(\frac{1}{m_a}+\frac{1}{m_b}\right)\Big/\left(\frac{T_a}{m_a}+\frac{T_b}{m_b}\right)}, \qquad (9) \end{aligned}$$

where the definition of the operators C_{ab}^{T0} and $\mathcal{P}_a$ are shown in Ref.[7]. Since C_{ab}^{T0} represents the pitch-angle and velocity scattering terms, it can be implemented by the random walk in the $(v = |\mathbf{v}|, \xi = v_\parallel/v)$ space in Monte Carlo way[13, 14]. The explicit form of C_{ab}^{T0} in the Monte Carlo simulation is explained in Appendix A. Let us consider the change in the distribution function δf_a by a time integral of short period Δt according to C_{ab}^{T0}, i. e., $\delta f_a^{(T0)} = \Delta t C_{ab}^{T0}\delta f_a^{(0)}$, where superscripts (0) and $(T0)$ denote the distribution function before and after operating the random walk, respectively. By using the adjointness and particle conservation of the operator C_{ab}^{T0}, time integral of the terms on the RHS of Eq. (8) can be approximately evaluated as follows:

$$\begin{aligned} \Delta t \mathcal{P}_a C_{ab}^{T0}\delta f_a &= f_{Ma}\left[\frac{m_a v_\parallel}{T_a}\Delta u_{ab}^{(T0)} + \frac{2}{3v_a^2}\left(x_a^2-\frac{3}{2}\right)\Delta E_{ab}^{(T0)}\right], \qquad (10) \\ \Delta t C_{ab}^{T0}\mathcal{P}_a\delta f_a &= \Delta t\left[\frac{m_a}{T_a}C_{ab}^{T0}(v_\parallel f_{Ma})\left\{\frac{\delta u_a^{(T0)}+\delta u_a^{(0)}}{2}\right\}\right. \\ &\quad \left. +C_{ab}^{T0}(x_a^2 f_{Ma})\left\{\frac{2}{3v_a^2}\left(\frac{\delta E_a^{(T0)}+\delta E_a^{(0)}}{2}\right)-\delta n_a^{(0)}\right\}\right], \qquad (11) \end{aligned}$$

$$\Delta t \mathcal{P}_a C_{ab}^{T0} \mathcal{P}_a \delta f_a = -\frac{\Delta t}{\tau_{ab}} \frac{4\alpha_{ab}}{3\sqrt{\pi(1+\alpha_{ab}^2)}} f_{Ma} \left[\frac{m_a v_\parallel}{T_a} \left(\frac{\delta u_a^{(T0)} + \delta u_a^{(0)}}{2} \right) + \frac{2}{1+\alpha_{ab}^2} \left(x_a^2 - \frac{3}{2} \right) \left\{ \frac{2}{3v_a^2} \left(\frac{\delta E_a^{(T0)} + \delta E_a^{(0)}}{2} \right) - \delta n_a^{(0)} \right\} \right] \quad (12)$$

where $x_a = v/v_a$, $\alpha_{ab} = v_a/v_b$, $\tau_{ab}^{-1} = n_b e_a^2 e_b^2 \ln\Lambda_{ab}/(4\pi m_a^2 \epsilon_0^2 v_a^3)$, and

$$\delta n_a^{(0)} = \int d^3v \ \delta f_a^{(0)} \left(= \int d^3v \delta f_a^{(T0)} \right), \quad (13)$$

$$\delta u_a^{(0,T0)} = \frac{1}{n_a} \int d^3v \ v_\parallel \delta f_a^{(0,T0)}, \quad (14)$$

$$\delta E_a^{(0,T0)} = \frac{1}{n_a} \int d^3v \ v^2 \delta f_a^{(0,T0)}, \quad (15)$$

$$\Delta u_{ab}^{(T0)} = \delta u_a^{(T0)} - \delta u_a^{(0)}, \quad (16)$$

$$\Delta E_{ab}^{(T0)} = \delta E_a^{(T0)} - \delta E_a^{(0)}. \quad (17)$$

Note here that $\Delta u_{ab}^{(T0)}$ and $\Delta E_{ab}^{(T0)}$ represents the change in δu_a and δE_a by C_{ab}^{T0}. Also note that the definition of τ_{ab}^{-1} in the present paper is $3\pi^{1/2}/4$ times of that in Ref.[7], and we use the MKS unit. The symbol $\parallel$ in the subscript of δu_a and Δu_{ab} are omitted here and hereafter. Since the velocity moments such as Eqs. (13)-(15) are easy to be evaluated in a particle δf code, numerical calculation of C_{ab}^T in the form Eqs. (10)-(12) is a convenient way to implement the test-particle operator than to implement the original form of C_{ab}^T by Sugama, Eqs (32) and (33) in Ref. [7], to a particle code.

In the two-weight δf method for drift-kinetic simulations[15, 16], distribution function is represented by the marker distribution function g and the marker weights (w, p) which satisfy the following relations:

$$\delta f = wg = \sum_i w_i \delta(\mathbf{v} - \mathbf{v}_i) \quad , \quad f_M = pg = \sum_i p_i \delta(\mathbf{v} - \mathbf{v}_i),$$

where the subscript i represents the index of simulation markers. Consider here the Monte Carlo operator $\Delta t C_{ab}^{T0}$ changes each marker's velocity $\mathbf{v}_i \to \mathbf{v}_i + \Delta\mathbf{v}_i$. Then, the change of δf_a by whole the test-particle part can be expressed formally as follows:

$$\delta f_a^{(T0)}(\mathbf{v}_i + \Delta\mathbf{v}_i) = \delta f_a^{(0)}(\mathbf{v}_i) + f_{Ma}(\mathbf{v}_i + \Delta\mathbf{v}_i)) \times S_{ab}^T \left[\delta n_a^{(0)}, \delta U_a^{(0)}, \delta u_a^{(T0)}, \delta E_a^{(0)}, \delta E_a^{(T0)}, \theta_{ab}; \mathbf{v}_i + \Delta\mathbf{v}_i \right], \quad (18)$$

where S_{ab}^T, which is a functional of velocity moments of δf_a before and after applying the random walk C_{ab}^{T0}, represents the three terms which is proportional to $(\theta_{ab}-1)$ in Eq.(8), and we have used the fact that $C_{ab}^{T0}(v_\parallel f_{Ma})$ and $C_{ab}^{T0}(x_a^2 f_{Ma})$ in Eq. (11) are known analytic functions (See Ref. [7]) which are proportional to $f_{Ma}(\mathbf{v})$. According to the source term S_{ab}^T, each marker weight w_i changes by $\Delta t C_{ab}^T$ as

$$w_i^{(T)} = w_i^{(0)} + (f_{Ma}/g) S_{ab}^T = w_i^{(0)} + p_i S_{ab}^T. \tag{19}$$

Note that the weight p_i does not change by the linearized collision operator, and S_{ab}^T vanishes if $T_a = T_b$ $(\theta_{ab}=1)$. In the following, we represent the distribution function after operating C_{ab}^T as $\delta f_a^{(T)}$.

Next let us consider the field-particle operator C_{ab}^F. Sugama's modified Landau operator for the field-particle term is made so as to satisfy both the conservation properties and adjointness nature, as follows:

$$\begin{aligned}
\Delta t C_{ab}^F(\delta f_b) &= f_{Ma}(v)\left[c_0 \delta N_{ab}^T \left(\frac{1}{n_a} - \frac{3Q_{ab}}{2}\right)\right. \\
&\quad \left. + c_1 \delta V_{ba}^T R_{ab}(v)\left(\frac{v_\parallel}{v_a}\right) + c_2 \delta W_{ba}^T Q_{ab}(v)\right], \qquad (20)\\
\delta N_{ab}^T &= \int_t^{t+\Delta t} dt \int d^3v C_{ab}^T(\delta f_a) \simeq \int d^3v [\delta f_a^{(T)} - \delta f_a^{(0)}], \qquad (21)\\
\delta V_{ba}^T &= \frac{1}{m_a v_a}\int_t^{t+\Delta t} dt \int d^3v \frac{\delta f_b}{f_{Mb}} C_{ba}^T(m_b v_\parallel f_{Mb}) \\
&= \frac{1}{m_a v_a}\int_t^{t+\Delta t} dt \int d^3v m_b v_\parallel C_{ba}^T(\delta f_b) \simeq \frac{n_b m_b}{m_a v_a}\Delta u_{ba}^{(T)}, \qquad (22)\\
\delta W_{ba}^T &= \frac{1}{T_a}\int_t^{t+\Delta t} dt \int d^3v \frac{\delta f_b}{f_{Mb}} C_{ba}^T\left(\frac{m_b v^2}{2} f_{Mb}\right) \\
&= \frac{1}{T_a}\int_t^{t+\Delta t} dt \int d^3v \frac{m_b v^2}{2} C_{ba}^T(\delta f_b) \simeq \frac{n_b m_b}{2T_a}\Delta E_{ba}^{(T)}, \qquad (23)\\
R_{ab}(v)\left(\frac{v_\parallel}{v_a}\right) &= f_{Ma}(v)^{-1}\frac{C_{ab}^T(\frac{v_\parallel}{v_a} f_{Ma})}{\int d^3v \frac{v_\parallel}{v_a} C_{ab}^T(\frac{v_\parallel}{v_a} f_{Ma})} \\
&= \left(\frac{v_\parallel}{v_a}\right)\frac{2\theta_{ab}(1+\alpha_{ab}^2)^{5/2}}{n_a \alpha_{ab}^3 (m_a/m_b+1)}\left[\frac{3\sqrt{\pi}G(x_b)}{2x_a}\right.
\end{aligned}$$

$$+\frac{\alpha_{ab}(\theta_{ab}-1)}{(1+\alpha_{ab})^{3/2}}\Bigg], \tag{24}$$

$$\begin{aligned} Q_{ab}(v) &= f_{Ma}(v)^{-1}\frac{C^T_{ab}(x_a^2 f_{Ma})}{\int d^3v x_a^2 C^T_{ab}(x_a^2 f_{Ma})} \\ &= \frac{2\theta_{ab}(1+\alpha_{ab}^2)^{5/2}}{3n_a\alpha_{ab}^3\,(m_a/m_b+1)} \\ &\quad\times\Bigg[\frac{3\sqrt{\pi}}{4\alpha_{ab}^2 x_a}\left\{\Phi(x_b)-x_b\Phi'(x_b)(1+\alpha_{ab}^2)\right\} \\ &\quad+\frac{\alpha_{ab}(\theta_{ab}-1)}{(1+\alpha_{ab}^2)^{3/2}}(x_a^2-3/2)\Bigg] \end{aligned} \tag{25}$$

where

$$\begin{aligned} \Delta u^{(T)}_{ba} &= \delta u^{(T)}_b - \delta u^{(0)}_b, \\ \Delta E^{(T)}_{ba} &= \delta E^{(T)}_b - \delta E^{(0)}_b, \end{aligned}$$

and $\Phi(x)$ and $G(x)$ are defined in the Appendix A. We have already modified the form of Eq. (20) from the original one in Ref.[7]. Also, the adjointness of C^T is used to derive Eqs. (22) and (23). In the ideal limit where there is no numerical error in evaluating velocity and time integrals in C^T_{ab}, δN^T_{ab} [note that it is not N^T_{ba} but N^T_{ab} which should appear in Eq.(20)] becomes zero and $(c_0, c_1, c_2) = (0, -1, -1)$ corresponds to the original form of C^F_{ab} in Ref.[7]. However, as it has been pointed out in previous studies on like- and unlike-collision operators[8, 11, 15, 17], direct numerical implementation of C^F_{ab} as in the original form fails to keep the conservation properties of collision operator because of the accumulation of numerical errors in the velocity and time integrals. Therefore, as we have adopted for like-particle collision operator in the previous FORTEC-3D[8] and in a continuum gyrokinetic full-f code GT5D[18], the numerical factors (c_0, c_1, c_2) are determined at each time when collision term is operated so that it ensures the conservation of particle number, momentum, and energy in the collisions between particle species a and b, i. e., Eqs. (2) and (3). The validity of the modified C^F_{ab} operator for the unlike-particle collisions will be confirmed later in the benchmark calculations.

Since Eq. (20) is proportional to f_{Ma}, it can be rewritten as $S^F_{ab} f_{Ma}$. Therefore, the field-particle operator act as a source term on marker weight w_i as in a similar way as S^T_{ab} from test-particle part. Therefore, in summary,

after operating whole the C_{ab}^T and C_{ab}^F terms, each marker's velocity $\mathbf{v}_i$ and weight w_i change as

$$\begin{aligned} \mathbf{v}_i(t+\Delta t) &= \mathbf{v}_i(t) + \Delta \mathbf{v}_i, \\ w_i(t+\Delta t) &= w_i^{(T)} + p_i S_{ab}^F = w_i^{(0)} + p_i (S_{ab}^T + S_{ab}^F). \end{aligned}$$

Note here that the collision operator should be evaluated and operated in the order $C^{T0} \to S^T \to S^F$ in the δf Monte Carlo simulation. Since S_{ab}^F requires information of change in momentum and energy of the opponent particle species b, $C_{ab}^L(\delta f_a)$ and $C_{ba}^L(\delta f_b)$ should be calculated at once. If there are three or more particle species, one needs to repeat the procedure for all the combination including like-particle collisions, (a,a), (a,b), (a,c), $\cdots$, (b,b), (b,c), $\cdots$ etc.

4. Benchmark of the collision operator

4.1. Benchmark with a full-f PIC code

To benchmark the modified linearized collision operator, firstly we compared the momentum and energy relaxation process between two ion species simulated by a different model of collision operator. Here we used a full-f PIC simulation code with Nanbu-model collision operator[12] to benchmark our δf Monte Carlo code. In a full-f code, the total distribution function $f_a = f_{Ma} + \delta f_a$ rahter than the perturbed part δf_a is represented by the simulation markers, of which weights are usually uniform. This is the main different point from the δf code in which markers have non-uniform weight. To simulate the Coulomb collision process by Nanbu model operator, it randomly chooses pairs of simulation markers in a tiny cell, and then evaluate the cumulative scattering angle of these two charged particles from the impact parameter and relative velocity. This collision operator is essentially nonlinear, while the linearized collision term neglects the $C_{ab}(\delta f_a, \delta f_b)$ term.

The benchmark has been carried out as follows. The initial distribution functions of particle species a and b were given as shifted Maxwellian as Eq. (7) with different initial perturbation amplitude $\delta u_a/v_a = 0.1$, $\delta u_b/v_b = -0.1$, $\delta T_a/T_a = 0.05$, $\delta T_b/T_b = -0.05$. Note that in the δf code, the initial simulation marker distribution g is given by random sampling of f_M and therefore the marker weight of particle species a is uniform, $p_a = f_{Ma}/g = n_a/N$, where N is the number of simulation markers. The initial shifted

Maxwellian is then represented by non-uniform initial weight w_{ai}:

$$w_{ai}(t=0) = p_a \left[\frac{\delta n_a}{n_a} + 2\frac{\delta u_a}{v_a} v_{\|i} + \frac{\delta T_a}{T_a} \left(\frac{m_a^2 v_i^2}{2T_a} - \frac{3}{2} \right) \right].$$

On the other hand, in the full-f PIC code, the initial simulation particles are loaded by the random sampling of the shifted Maxwellian in the following form,

$$f_{SMa} = (n_a + \delta n_a) \left(\frac{m_a}{2\pi(T_a + \delta T_a)} \right)^{3/2} \exp \left[-\frac{m_a(\mathbf{v} - \delta \mathbf{u}_{\|a})^2}{2(T_a + \delta T_a)} \right].$$

The difference in the initial distribution between the δf code and the full-f PIC code is negligibly small, $\mathcal{O}(\delta^2)$.

To test the mass-ratio dependence, the particle species a was chosen as H^+ while b was varied (D, T, C, Ar, Fe, Kr, Ag, W). The ion charge of species b and $\ln \Lambda_{ab}$ were fixed to +2 and 18 respectively, for simplicity. The other parameters were : $n_a = 1 \times 10^{19}[\mathrm{m}^{-3}]$, $n_b = 0.5 \times 10^{19}[\mathrm{m}^{-3}]$, $T_a = T_b = 2[\mathrm{keV}]$, $\delta n_a/n_a = \delta n_b/n_b = 0.1$. Note here that the Nanbu operator in full-f PIC code contains the slow energy equilibration process among two Maxwellians $C_{ab}(f_{Ma}, f_{Mb})$ if $T_a \neq T_b$, while it is neglected in the δf code. Therefore, here we compared the two simulation codes in $T_a = T_b$. In these benchmark calculations $N_m = 2 \times 10^5$ markers per one species were used in both two codes. The time step size in the δf code is determined by τ_{min}, which is the minimum value of $\tau_{ij}(i, j = a \text{ or } b)$ in each case. In the present benchmarks, $\Delta t = 5 \times 10^{-4} \tau_{min}$ was chosen.

Figures 1 and 2 show the time evolution of the parallel mean flow $\delta u = n^{-1} \int d^3v v_{\|} f$ and temperature fluctuation $\delta T/T = n^{-1} \int d^3v (mv^2/(3T) - 1) f$. It was found that the damping rate of δu and $\delta T/T$ of both species a and b agreed well between δf Monte Carlo code and the full-f PIC code. One can see that the final stationary state satisfies the condition $\delta u_a \simeq \delta u_b$ and $\delta T_a/T_a \simeq \delta T_b/T_b$, as it is expected from the H-theorem. Here, the expectation values of δu and $\delta T/T$ at $t \to \infty$ can be evaluated from the initial values, by using the conservation of total momentum and energy, as

$$\begin{aligned} \delta u(t \to \infty) &= \frac{\sum_a m_a n_a \delta u_a(t=0)}{\sum_a m_a n_a}, \\ \frac{\delta T}{T}(t \to \infty) &= \frac{\sum_a n_a \delta T_a(t=0)}{\sum_a n_a T_a}. \end{aligned} \tag{26}$$

The convergence of the δf simulation was checked by varying the number of simulation markers as shown in Table 1 for the H-Fe case. It was confirmed that the δu and $\delta T/T$ in the simulations converged to their expectation values, and the standard deviation was roughly proportional to $1/\sqrt{N_m}$. Therefore, we conclude that both simulation methods correctly simulate the damping process of distribution function towards the stationary state. The statistic noise on δu and $\delta T/T$ is larger in the PIC simulation than that in δf simlation, especially on $\delta T/T$. The fluctuation is caused by the sampling noise of distribution function by finite number of markers. Since the markers in δf method is used for sampling only the small perturbation part of distribution function, δf, it is expected that the sampling noise level in a δf simulation is $\mathcal{O}[(\delta f/f_M)^2]$ smaller than that in a full-f method if they use the same number of simulation markers[19]. This is the advantage of the δf scheme. However, δf method cannot be applied to a far-nonequilibrium system where $\delta f/f_M \sim \mathcal{O}(1)$ such as SOL/divertor region of torus plasmas, and the full-f method is indispensable to simulate the kinetic transport process in such a case.

Table 1: Time average and standard deviation of δu and $\delta T/T$ (H-Fe case) evaluated from t=$175\tau_{min}$ to $250\tau_{min}$. The theoretical expectation values are obtained from Eq. (26).

Marker Number N_m	δu_H[km/s]	$\delta u_{Fe}[km/s]$	$\delta T_H/T_H(\times 100)$	$\delta T_{Fe}/T_{Fe}(\times 100)$
48000	-5.545± 1.717	-5.832± 0.061	1.834± 0.099	1.399± 0.197
192000	-5.903± 0.821	-5.874± 0.029	1.711± 0.057	1.583± 0.114
768000	-5.962± 0.381	-5.850± 0.014	1.649± 0.031	1.679± 0.062
3072000	-5.800± 0.191	-5.856± 0.007	1.690± 0.032	1.662± 0.063
Expectation	-5.852	-5.852	1.667	1.667

In figures 1 and 2, it is found that the momentum transfer between two species completes in the time scale of $10\tau_{min}$, while the energy equilibration time becomes slower as the mass ratio m_b/m_a is larger. Therefore, when one carries out a neoclassical transport simulation which includes several ion species with separated masses, it will take long time steps until it reaches a quasi-steady state and the accumulation of numerical error in particle number $\delta N \equiv \sum_a |\delta n_a|$, total momentum $\delta P \equiv \sum_a m_a n_a \delta u_a$, and total kinetic energy $\delta K \equiv \sum_a (m_a n_a/2)\delta E_a$ in the long-term simulation might be a problem. Here, δn, δu, and δE are defined in Eqs. (13)-(15). Strictly speaking, the

conservation of plasma particle number should be satisfied in each particle species δn_a independently. However, we check the conservation property of particle number by summing up the absolute values of δn_a for simplicity. Figure 3 shows the time evolution of accumulated relative error in $|\delta N|$, $|\delta P|$, and $|\delta K|$ in the δf simulation for the three cases ($a = H, b =$C, Fe, and W). If the correction scheme in the field-particle operator is turned on, the coefficients ($c_0,\ c_1,\ c_2$) in Eq. (20) are determined so that the linearized collision operator $C^T_{ab} + C^F_{ab}$ should satisfy the conservation properties, Eqs. (2) and (3), among the all combination of two particle species including like-particle collisions. In Fig. 3, it is clearly demonstrated that the correction scheme kept the relative error in $|\delta N|$, $|\delta P|$, and $|\delta K|$ within the rounding-error level, and no accumulation of numerical error happened up to 100 collision times. On the other hand, if the correction scheme was turned off, the relative error in conserved quantities became $\mathcal{O}(0.01)$. Though the numerical error level can be reduced by increasing the number of simulation markers as shown in Table 1, the correction scheme suppresses the numerical error very efficiently. Figure 4 is the comparison of the time evolution of δu between with and without the correction term in C^F_{ab}. It demonstrates that the correction term has no side effect on the time evolution of mean flow towards the steady state solution. We have also checked that the correction scheme does not affect the time evolution of $\delta T/T$.

It should be noted that the correction scheme compels the C^F_{ab} operator to satisfy the conservation properties of linearized operator, even if there is any mistake or large error in C^T_{ab} or C^F_{ab} themselves. To verify the correction scheme, we investigated how the correction coefficients c_i in Eq. (20) behaved. In Figure 5, the distribution of $(|1 + c_1|, |1 + c_2|)$ for C^F_{ab} during the simulations for $(a, b) =$(H,C), (H, Fe), and (H,W) plasmas are shown. In the ideal limit c_1 and c_2 should converge to -1. As the number of simulation markers increases, $(|1 + c_1|, |1 + c_2|)$ was found to approach to $(0, 0)$ as it is expected. We also found that the coefficient c_0 also remained small, $\mathcal{O}(0.01 \sim 0.1)$, during the simulations. Therefore, it is verified that the collision operators C^T_{ab} and C^F_{ab} are correctly implemented. As the mass ratio m_b/m_a becomes larger, $|1 + c_2|$ tends to spread in wider range $0.0001 \sim 0.1$ than $|1 + c_1|$ even if we use many simulation markers. It is inferred that the statistic noise from the random-walk part in C^{T0}_{ab} tends to affect the conservation property when $m_a/m_b \ll 1$. We will discuss on this point later in Summary.

4.2. Benchmark with a continuum gyrokinetic δf code

Next, to check the adjointness of the collision operator and the H-theorem in the case of different temperatures, we carried out simulations of a 4-species plasma (D^+, T^+, He^{+2}, C^{+6}) by the δf Monte Carlo code and compared the result with the same Sugama operator implemented in a continuum gyrokinetic δf code[11]. The initial plasma parameters are shown in Table 2. Time step size in the δf Monte Carlo simulation was set to $\Delta t = 2.5 \times 10^{-4} \tau_{min}$ where $\tau_{min} = \tau_{CC}$ in this case, and the number of simulation markers per species was $N_m = 4.8 \times 10^5$.

First, let us compare the time evolution of mean flow δu and the temperature perturbation $\delta T/T$ from the two codes. As shown in Figure 6, the damping rate and the final steady state values of δu and $\delta T/T$ agreed very well between two codes. It took $t \sim 150\tau_{CC}$ to reach to a stationary state where all the δu_a and $\delta T_a/T_a$ of four species converge to the same value, as it is expected. Thus it is verified that the Sugama's modified operator works correctly in the Monte Carlo code for multi-ion-species cases.

Table 2: Parameters in the 4-species plasma simulation

	D	T	He	C
Charge Z_a	+1	+1	+2	+6
Mass m_a	2	3	4	12
Density n_a [$10^{19}\mathrm{m}^{-3}$]	1.00	1.00	0.10	0.04
Temp. T_a [keV]	2.0	2.2	1.8	1.8
initial $\delta n_a/n_a$	0.10	0.10	0.10	0.05
initial $\delta u_a/v_a$	0.10	-0.10	0.10	-0.20
initial $\delta T_a/T_a$	0.05	-0.05	-0.10	0.10

Second, for the benchmark of the H-theorem in a plasma including 3 or more particle species, it is more convenient to observe the time evolution of the following quantities δH_a and their sum H than directly checking the relation Eq.(6),

$$\begin{aligned} \frac{dH}{dt} &= \sum_a T_a \sum_b \int d^3v \frac{\delta f_a}{f_{Ma}} C_{ab}(\delta f_a) \\ &= \sum_a \frac{T_a}{2} \frac{d}{dt} \int d^3v \frac{\delta f_a^2}{f_{Ma}} \equiv \sum_a \frac{T_a}{2} \frac{d}{dt} \delta H_a \leq 0. \end{aligned} \tag{27}$$

In Figure 7(a), the time evolution of $(T_a/n_a)\delta H_a$ in the Monte Carlo simulation is plotted. Unexpectedly, δH_a of all the four species, and therefore their sum H, increased monotonously after $t > 30\tau_{CC}$, and the increase continued even after δu and $\delta T/T$ reached the stationary state, $t > 150\tau_{CC}$. This tendency, which contradicts to the H-theorem, has been pointed out by Brunner[16] in the discussion on the "weight speading" problem caused by the Monte Carlo collision operator for the two-weight δf method. Because of the approximation of the test-particle operator C_{ab}^{T0}, which is originally the second-order partial differential equation [Eqs. (3), (4) and (27) in Ref.[7]], by the Langevin equation-like random walk of simulation markers in the velocity space, the weight w_i of each marker tends to spread from its ensemble average value, $\overline{W}(\mathbf{v})$, i. e., $w_i(\mathbf{v}_i) = \overline{W}(\mathbf{v} = \mathbf{v}_i) + \tilde{w}_i$. Note here that the ensemble average value of $\tilde{w}_i$ over all markers is zero. Then, the numerical evaluation of δH_a in the δf Monte Carlo code becomes

$$\begin{aligned} \delta H_a &= \int d^3v \frac{\delta f_a^2}{f_{Ma}} \simeq \sum_i \frac{w_{a,i}^2}{p_{a,i}} \\ &= \sum_i \frac{\overline{W}(\mathbf{v}_i)^2}{p_i} + \sum_i \frac{\tilde{w}_i^2}{p_i}, \end{aligned} \tag{28}$$

where the subscript a to represent the particle species has been suppressed in the second line. Note that since the linearized collision operator does not change the weight p_i, one should consider only the weight spreading of w in the present case. Though the ensemble average part, $\delta\bar{H}_a = \sum_i \overline{W}(\mathbf{v}_i)^2/p_i$, obeys the H-theorem and $\sum_a \delta\bar{H}_a$ is a decreasing function, the contribution from the $\tilde{w}_i^2$-part increases proportionally to time t, as Brunner has pointed out. This apparent breaking of H-theorem by weight spreading can be restored by the weight averaging method which has also been developed by Brunner in the same reference. Actually, FORTEC-3D code for single-species plasma has already adopted the weight averaging method[20]. In the simulation shown in Fig. 6 and Fig. 7(a), the weight averaging has been turned off intentionally to see the effect of weight spreading on H-theorem. If the weight averaging is turned on, the marker weights are modified as follows; (the details of the definition of the average weight field $W_a(\mathbf{v})$ is described in [16, 20])

$$w_i' = \gamma_a W_a(\mathbf{v}_i) + (1 - \gamma_a) w_i, \tag{29}$$

where the damping rate γ_a is controlled by a input parameter f_W as follows:

$$\gamma_a \equiv 1 - \exp(-\Delta t f_W/\tau_{aa}), \tag{30}$$

so that the variance of marker weight $\tilde{w}^2$ damps exponentially in the time scale of τ_{aa}/f_W. Larger f_W means stronger averaging on the marker weights. Figure 7(b) shows the dH_a in the simulations with $f_W = 1$ (modest weight averaging case) and $f_W = 5$ (strongly averaging case), as well as those evaluated in the gyrokinetic simulation. It should be noted here that the gyrokinetic δf code is free from the weight-spreading problem, since it is not a Monte Carlo code. In the figure, one can see that δH_a of four species decreased with time by adopting the weight average scheme, and they converged to a stationary values at $t > 150\tau_{CC}$, when δu_a and $\delta T_a/T_a$ reached to a steady state. Thus the H-theorem, $dH/dt = \sum_a T_a(d\delta H_a/dt) \leq 0$, was restored and $d(\delta H_a)/dt \to 0$ as $t \to \infty$. As the strength of weight averaging f_W increases, the time evolution and the steady state values of δH_a approaches to those observed in the continuum gyrokinetic simulation. It is then confirmed that the weight averaging method correctly remove the contribution of the $\tilde{w}^2$-part to δH_a in Eq.(28).

Though it is demonstrated that the weight averaging method works well to recover the H-theorem, one may be afraid of possible side effect of the weight averaging method in transport simulation. Therefore, we checked the dependence of several quantities on the strength of avaraging, f_W. In Figure 8(a) to (d), time average values of δu_a and so on between $t = 250$ to $300\tau_{CC}$ are compared among the simulations with f_W varied from 0 (no averaging) to 5. Since the weight averaging method is constructed so as to conserve the particle number, momentum, and energy, it does not deteriorate the conservation property of δN, δP, δK (the same quantities as in Fig. 3) as shown in Fig. 8(a). In 8(b) and (c), time average of δu_a and $\delta T_a/T_a$ are compared. Here, the error bar is estimated from the standard deviation. It is found that if the weight averaging is turned off or very weak, the average values of δu_a and $\delta T_a/T_a$ deviate from the expectation values of them, and the error bars become larger for heavier ion species (He and C). By applying the weight averaging with enough strength ($f_W \geq 1.0$), the error level in δu and $\delta T/T$ reduced and converged to their expectation values. In Fig. 8(d) we checked the temperature anisotropy

$$\delta T_{\parallel a}/\delta T_{\perp a} = \int d^3v v_\parallel^2 \delta f_a / \int d^3v (v_\perp^2/2)\delta f_a.$$

Again, it is found that the error level in $\delta T_{\parallel a}/\delta T_{\perp a}$ is larger for heavier ions but can be suppressed by weight averaging. In Figs. 8 (a)-(d), the simulation results of $f_W = 1$ without using the correction scheme in C^F_{ab} for the conservation property are also shown for the purpose of comparison. As we have found in the 2-species simulations in Section 4.1, the correction of the field-particle operator does not affect the stationary-state average values of δu and δT but effectively reduces the accumulation of error in the quantities δN, δP, and δK.

To summarize, adopting the weight averaging method improve the S/N ratio in evaluating the velocity moments of δf without deteriorating the conservation property of particle numbers, momentum, and energy. It also serves to restore the H-theorem. Moreover, it was demonstrated that the weight-averaging scheme and the correction scheme in the field-particle operator to keep the conservation property can coexist. However, it should be noted that, in the actual application of the δf Monte Carlo method for neoclassical transport simulation, too mush strong averaging results in virtual increase of collision frequency. In torus plasmas especially in low-collisionality condition, there appears a localized variation of δf near the trapped-passing orbit boundary in the velocity space. Strong weight averaging will smooth out the large variation of δf across the boundary, and it will affect the evaluation of the neoclassical fluxes, too. According to the experience of neoclassical transport simulations by single-species FORTEC-3D code, a practical criterion of the strength of averaging without side effect is $f_W = 0.5 \sim 2.0$.

Finally, the adjointness of the linearized collision operator was tested in the following way. Since the adjointness property of the test-particle operators C^{T0} and C^T is difficult to check numerically in the Monte Carlo calculation, we checked the adjointness of the field-particle operator C^F, Eq.(5). It should be noted that the adjointness relations of C^{T0} and C^T are utilized in the derivation of the numerical representations of C^T and C^F, in Eqs. (10), (22) and (23), respectively. If the change of δf_a by the field-particle part is expressed formally as $(d/dt)|_{C^F_{ab}}\delta f_a$, time integral of [LHS of Eq.(5) − RHS of Eq.(5)] is numerically evaluated as

$$\Delta A^F_{ab} \equiv \int_t^{t+\Delta t} dt \left[T_a \int d^3v \frac{\delta f_a}{f_{Ma}} \left.\frac{d}{dt}\right|_{C^F_{ab}} \delta f_a - T_b \int d^3v \frac{\delta f_b}{f_{Mb}} \left.\frac{d}{dt}\right|_{C^F_{ba}} \delta f_b \right] \Bigg/ \left| T_a \int d^3v \frac{\delta f_a^2}{f_{Ma}} \cdot T_b \int d^3v \frac{\delta f_b^2}{f_{Mb}} \right|^{1/2}$$

$$\simeq \left[T_a \int d^3v \left\{ \frac{\delta f_a^{(F)2}}{f_{Ma}} - \frac{\delta f_a^{(T)2}}{f_{Ma}} \right\} - T_b \int d^3v \left\{ \frac{\delta f_b^{(F)2}}{f_{Mb}} - \frac{\delta f_b^{(T)2}}{f_{Mb}} \right\} \right] \Bigg/ \left| 2T_a \int d^3v \frac{\delta f_a^{(F)2}}{f_{Ma}} \cdot T_b \int d^3v \frac{\delta f_b^{(F)2}}{f_{Mb}} \right|^{1/2}, \quad (31)$$

which is normalized in a similar way as $\Delta_{ab}^{(adj)F}$ in Refs. [10, 11]. Here, $\delta f_a^{(T)}$ and $\delta f_a^{(F)}$ represent the distribution function after operating only the C_{ab}^T part and after operating both $C_{ab}^T + C_{ab}^F$ parts, respectively. ΔA_{ab}^F evaluates the relative numerical error in the adjointness of C_{ab}^F per one operation of C_{ab}^F. For like-particle collisions, $\Delta A_{aa}^F = 0$ by definition. Figure 9 shows the average and standard deviation of ΔA_{ab}^F for unlike-particle collisions in the 4-species plasma simulation. Note that these are the case with the time step size $\Delta t = 2.5 \times 10^{-4} \tau_{CC}$ and $N_m = 4.8 \times 10^5$ per a species, except for the "$N \times 4$" case in the figures. The effect of tuning on/off the correction scheme in C_{ab}^F to maintain the conservation property was also compared for the case of $f_W = 1$. It is found that the average and standard deviation of ΔA_{ab}^F are $O(10^{-9} \sim 10^{-7})$ and $O(10^{-9} \sim 10^{-6})$, respectively, and the amplitude tends to be larger for the combination of larger mass ratio such as (a, b) =(D,C) and (T,C). The adaptation of the strong weight averaging ($f_W \geq 1$) resulted in increasing the standard deviation of ΔA_{ab}^F about factor 2 but the fluctuation was still remain small, $< 10^{-6}$, and it became smaller if the number of simulation markers was increased. It should be pointed out that, though the complete adjointness nature of the field-particle operator as Eq. (5) is broken when the correction scheme in C_{ab}^F is adopted, it did not affect in practice on the error level of the adjointness of the C_{ab}^F operator. Though the error level of ΔA_{ab}^F is larger than that of δN, δP and δK (error in conservation of particle number, momentum, and kinetic energy), the adjointness property of the field-particle operator is proved to be realized with enough accuracy in the numerical simulation.

5. Summary

In this paper, a numerical method of the linearized Coulomb collision operator for multi-ion-species plasmas in particle-base δf Monte Carlo code have been presented, which satisfies the adjointness of the operator and the H-theorem even if the particle species have different temperatures. In the benchmarks between a full-f PIC code which uses Nanbu-model Monte Carlo

collision term and a δf continuum gyrokinetic code which uses the same modified Landau operator constructed by Sugama, it has been demonstrated that the processes of the damping of the mean flow and the thermalization of each particle species towards a stationary state agree well with one another. The conservation properties of particle number, momentum, and energy of the linearized operator were satisfied with high accuracy, within the rounding error level. Thus the numerical method to implement Sugama's modifield collision oparator in a δf Monte Carlo code has been verified. It is found that the weight-spreading phenomenon happening in the δf code deteriorates the reproducibility of the H-theorem numerically, and this can be restored by adopting the weight-averaging method which is already used in the δf neoclassical transport code, FORTEC-3D.

The motivation of developing the numerical method of multi-ion-species collision operator is to contruct a neoclassical transport simulation code for nuclear fusion reactors. To evaluate the neoclassical radial particle and energy fluxes as well as bootstrap current in multi-species plasmas, it is expected that the δf simulation code should solve the time integral of drift-kinetic equation up to several tens times of collision time, τ_{ab}, which varies according to the combination of particle species (a, b). As the mass ratio of two paricles species becomes larger, the thermalization process becomes slower and it requires longer time steps of simulation to reach a steady-state solution. Also, the large mass ratio allows that ion species have small but finite different temperature. The present collision operator which satisfies the conservation property and the H-theorem forms the reliable basis for such a long-duration neoclassical transport simulation for multi-species plasmas.

It is several remaining issues we have not considered here to develop such a multi-species neoclassical transport code. First, it is required to consider the Coulomb logarithm for unlike-species collisions, $\ln \Lambda_{ab}$. Throughout this article, we have used the constant value of $\ln \Lambda_{ab} = 18$ for simplicity, but $\ln \Lambda_{ab}$ and therefore the collision time τ_{ab} vary about $10 \sim 20\%$ accoring to the analytic models for $\ln \Lambda_{ab}$. We will adopt the analytic model proposed by Honda[21] which is applicable for wide range of plasma parameters. The second probrem is the increase in the calculation time in multi-species collision operator. Since one needs to solve whole the combination of the species contained in a plasma, the computation cost for N-species plasma is about N^2 times of that required in a single-species case. Therefore, it is preferable that the collision opearator calculation is parallelized. Also, the amount of random numbers required in N-species plasma incleases N^2 times. How-

ever, since we have already implemented the parallel pseudo-random number generation scheme of Mersenne Twister[22, 23] in our transport code, the increase in the time cost of random number generation can be negligible. To speed up the multi-species linearized collision operator, we have tested running the present Monte Carlo code on the Intel Phi accelerator in HELIOS system of IFERC-CSC, Rokkasho, Japan using the native mode. However, the present test code for collision operator uses many MPI ALLREDUCE communication among the MPI ranks to evaluate integrals such as Eqs. (14) and (15). When the code was running in parallel on the Phi accelerator, the collective communication became the bottleneck of computation, and therefore the efficient computation on Phi accelerators compared to the same code running on the main Xeon CPUs have not achieved yet. To achieve a high parallel computation efficiency in the Monte Carlo collision term, more elaborate algorithm should be adopted. For example, while a main CPU solves the collisions between a-b and b-a species, a Phi accelerator solves the c-d and d-c collisions, which is completely independent of the a-b collisions. Concealment of communication time behind another computation will be also an effective way.

Finally, in this article we have not tested the linearized collision operator for electron-ion case. As it is explained in the Appendix, the present Monte Carlo test-particle operator C_{ab}^{T0} has a numerical problem when the velocity of simulation marker is slow, $x_a \simeq 0$, and the ratio of thermal velocity of two species are large, $\alpha_{ab} = v_a/v_b \gg 1$. The main cause of the numerical problem is because the pitch-angle and energy diffusion collision frequency ν_D^{ab} and ν_v^{ab} are function of v. If $\alpha_{ab} \gg 1$, the numerical problem cannot easily be resolved by simply reducing the time step size Δt. A similar problem has also been reported in the continuum gyrokinetic δf code which adopts Sugama's modified operator for electron-ion collision case[11]. Though the present Monte Carlo method works properly for the ion-ion collisions with large mass ratio such as H-Fe or H-W as it was demonstrated, it was found that larger correction is required in C_{ab}^{F} to keep the conservation properties as the mass-ratio becomes larger, as shown in Fig. 5. To treat the electron-ion collisions in the Monte Carlo neoclassical transport, we will have to adopt the large-mass-ratio approximation collision operator to avoid the numerical problem at $x_a \simeq 0$. The numerical way to Sugama's modified operator in the large-mass-ratio limit, which is also constructed to satisfy the adjointness of the operator, will be reported in another paper.

Acknowledgment

Part of the simulation was carried out using the HELIOS supercomputer system at International Fusion Energy Research Centre, Aomori, Japan, under the Broader Approach collaboration between Euratom and Japan, implemented by Fusion for Energy and JAEA. It was also carried out using Plasma Simulator in NIFS, under the auspices of the NIFS Collaboration Research programs (NIFS15KNST079, NIFS14KNTT026).

Appendix A. Implementation of the test-particle operator C_{ab}^{T0} in the Monte Carlo method

Although the numerical implementation of the test-particle collision operator in Monte Carlo codes appears in many articles, here we would like to present explicitly how the random walks of simulation markers in the velocity space $(v_i'^2, \xi_i') = (v_i^2 + \Delta v_i^2, \xi_i + \Delta\xi_i)$ are given in the C_{ab}^{T0} operator in our simulation code, for the readers' sake.

The original form of C_{ab}^{T0} is[7, 13]

$$\begin{aligned} C_{ab}^{T0}(\delta f_a) &= \nu_D^{ab}(v)\mathcal{L}\delta f_a + \mathcal{C}_v^{ab}(\delta f_a) \\ &= \frac{\nu_D^{ab}(v)}{2}\frac{\partial}{\partial\xi}\left[(1-\xi^2)\frac{\partial}{\partial\xi}\right]\delta f_a \\ &\quad + \frac{1}{v^2}\frac{\partial}{\partial v}\left[v^2\nu_v^{ab}(v)\left(v\delta f_a + \frac{v_a^2}{2}\frac{\partial}{\partial v}\delta f_a\right)\right], \end{aligned} \tag{A.1}$$

where we use $(v = |\mathbf{v}|, \xi = v_\parallel/v)$ as the velocity variables. Note that Eq. (A.1) is already averaged over the gyro-phase. The first and second terms represent the Lorentz pitch-angle scattering term and the energy diffusion term, respectively, and

$$\begin{aligned} \nu_D^{ab}(v) &= \tau_{ab}^{-1}\frac{\Phi(x_b) - G(x_b)}{x_a^3}, \\ \nu_v^{ab}(v) &= \tau_{ab}^{-1}\frac{2G(x_b)}{x_a}, \\ \Phi(x) &= \frac{2}{\sqrt{\pi}}\int_0^x dt\ \exp(-t^2), \\ G(x) &= \frac{\Phi(x) - x\frac{d}{dx}\Phi(x)}{2x^2}, \\ \tau_{ab}^{-1} &= n_b e_a^2 e_b^2 \ln\Lambda_{ab}/(4\pi m_a^2\epsilon_0^2 v_a^3). \end{aligned}$$

Note here that $x_a \equiv v/v_a$ and $x_b \equiv v/v_b$. In a Monte Carlo simulation, the random walk of $(\Delta v^2, \Delta\xi)$ of each marker velocity is given so that the time change in the average and the variance of (v^2, ξ) equal to those expected from Eq. (A.1). For example, by substituting $\delta f_a(\mathbf{v} = \mathbf{v}_i) = \delta(v - v_i)\delta(\xi - \xi_i)$, the expectation values of the changes in v^2 and v^4 of the markers at $v = v_i$ can be estimated as follows:

$$\begin{aligned}
\left\langle \frac{\Delta v^2}{\Delta t} \right\rangle &= \int d^3v\ v^2 \mathcal{C}_v^{ab}(\delta f_a) \\
&= -2\int d^3v\ v^2 \nu_v^{ab}\delta f_a + v_a^2 \int d^3v\ \delta f_a \left(3\nu_v^{ab} + v\frac{\partial}{\partial v}\nu_v^{ab}\right) \\
&= \nu_v^{ab}(v_i)v_i^2\left(-2 + 3\frac{v_a^2}{v_i^2}\right) + v_i v_a^2 \frac{\partial}{\partial v}\nu_v^{ab}(v_i) \\
&= -2\nu_v^{ab}(v_i)v_i^2\left[1 - \frac{\alpha_{ab}^2 \frac{d}{dx_b}\Phi(x_b)}{2x_b G(x_b)}\right]. \qquad \text{(A.2)} \\
\left\langle \frac{\Delta v^4}{\Delta t} \right\rangle &= \int d^3v\ v^4 \mathcal{C}_v^{ab}(\delta f_a) \\
&= \nu_v^{ab}(v_i)v_i^2\left(-4v_i^2 + 10v_a^2\right) + 2v_i^3 v_a^2 \frac{\partial}{\partial v}\nu_v^{ab}(v_i). \qquad \text{(A.3)}
\end{aligned}$$

From these equations, one can estimate the variance of v^2 as follows.

$$\begin{aligned}
\left\langle \frac{\Delta\sigma_{v^2}^2}{\Delta t} \right\rangle &= \left\langle \frac{\Delta v^4}{\Delta t} \right\rangle - \left\langle \frac{(\Delta v^2)^2}{\Delta t} \right\rangle = \left\langle \frac{\Delta v^4}{\Delta t} \right\rangle - 2v^2 \left\langle \frac{\Delta v^2}{\Delta t} \right\rangle \\
&= 4\nu_v^{ab}(v_i)v_i^2 v_a^2. \qquad \text{(A.4)}
\end{aligned}$$

Then, the $\mathcal{C}_v^{ab}(\delta f_a)$ operator is modeled as a Langevin equation of the simulation marker velocity,

$$\Delta v_i^2 = -\gamma_{v^2}^{ab}(v_i)v_i^2\Delta t + \delta R\sqrt{D_{v^2}^{ab}(v_i)\Delta t}, \qquad \text{(A.5)}$$

where $\gamma_{v^2}^{ab}(v_i) = -[\text{Eq. (A.2)}]/v_i^2$ is the friction coefficient, $D_{v^2}^{ab}(v_i) = [\text{Eq. (A.4)}]$ is the diffusion coefficient, and δR is a random number of which average is zero and the standard deviation is unity. In our calculation, δR is simply ± 1 with equal probability. It should be noted that we treat the random walk not in v, but in v^2 here. The reason is that, if we derive a Langevin equation for Δv as Eq. (A.5), then the drag force term $\gamma_v^{ab} v\Delta t$ diverges at $v \to 0$

and is difficult to treat numerically. One can construct the representation of random walk of $\Delta\xi$ by following the same way as in Eq. (A.2) - (A.5). The result is,

$$\begin{aligned} \Delta\xi_i &= -\gamma_\xi^{ab}(v_i)\xi_i\Delta t + \delta R\sqrt{D_\xi^{ab}(\mathbf{v}_i)\Delta t}, \qquad \text{(A.6)} \\ \gamma_\xi^{ab}(v_i) &= \nu_D^{ab}(v_i), \\ D_\xi^{ab}(\mathbf{v}_i) &= (1-\xi_i^2)\nu_D^{ab}(v_i). \end{aligned}$$

In the practical use, an important property that the Monte Carlo pitch-angle scattering operator (A.6) have is that if $|\xi_i| < 1$, then the range of the map $\xi_i' = C_{ab}^{T0}(\xi_i)$ is also bounded to $|\xi_i'| < 1$. One should note that the range of the map is not same as the domain of definition: $\xi_i \in [-1, +1]$, but is smaller than the domain, i. e., $\xi_i' \in [-1+\epsilon_\xi, +1-\epsilon_\xi]$, where $\epsilon_\xi = 0.5\nu_D^{ab}\Delta t$[13]. Therefore, the Monte Carlo pitch-angle scattering operator is correct only if $\nu_D^{ab}\Delta t \ll 1$. However, this condition is not always satisfied in multi-species plasma simulations using a common Δt for the time integral of all the simulation markers. It should be emphasized that the Δt for the collision operator should be the same value for all the markers of all particle species, because the present Monte Carlo collision operator involves the velocity integrals $\delta u_a^{(T0)}$ and $\delta E_a^{(T0)}$ as Eqs. (14) and (15) to evaluate the change in the momentum and energy by C_{ab}^{T0}, and also because the a-b and b-a collisions should be treated at once in the field-particle operator to satisfy the momentum and energy conservation. In our Monte Carlo code, for example, chooses $\Delta t \sim 10^{-4}\tau_{min}$ where τ_{min} is the minimum value of τ_{ab} from all the combination of the species (a, b). No matter how one chooses a small Δt, there is a finite probability that $\nu_D^{ab}(v_i)\Delta t \sim 1$, because the simulation markers have the velocity distribution close to Maxwellian, and $\nu_D^{ab}(v \to 0) \simeq 0.752\tau_{ab}^{-1}\alpha_{ab}x_a^{-2}$. However, it is not efficient to reduce the time step size for all the species only for the small fraction of markers which violates the condition $\nu_D^{ab}\Delta t \ll 1$. Instead, our strategy is that if $\nu_D^{ab}(v_i)\Delta t \sim 1$ for a simulation marker, then the test-particle operator C_{ab}^{T0} gives a random value of $\xi_i' \in [-1, +1]$, to mimic a large-angle pitch angle scattering. If Δt is chosen small enough, this treatment does not affect the simulation result. For example, in the 4-species plasma simulation shown in 4.2, where we choose $\Delta t = 2.5 \times 10^{-4}\tau_{min}$, only $10^{-4}\%$ of total test-particle collisions met the criterion $\nu_D^{ab}\Delta t > 1$.

For the energy diffusion term C_v^{ab}, the problem at $v \to 0$ is more complicated than the Lorentz operator, because ν_v^{ab} is a function of v in itself.

Considering the Taylor expansion of $\nu_v^{ab}(v)$ at $v \simeq 0$, one finds that

$$\nu_v^{ab}(v \simeq 0) \simeq \frac{4\alpha_{ab}}{3\sqrt{\pi}\tau_{ab}}, \tag{A.7}$$

$$v_i'^2(v_i \simeq 0) \simeq v_i^2\left[1 - \frac{8\alpha_{ab}\delta_{ab}}{3\sqrt{\pi}}\right] + v_a^2\frac{4\alpha_{ab}\delta_{ab}}{\sqrt{\pi}} + 4v_a v_i \delta R\sqrt{\frac{\alpha_{ab}\delta_{ab}}{3\sqrt{\pi}}}, \tag{A.8}$$

where $\delta_{ab} \equiv \Delta t/\tau_{ab}$. It should be noted that the approximation above is correct only if $\alpha_{ab}\delta_{ab} \ll 1$. From Eq. (A.8) one notices that

$$v_i'^2(v_i \to 0) = v_a^2\frac{4\alpha_{ab}\delta_{ab}}{\sqrt{\pi}}, \tag{A.9}$$

which means that, if $\alpha_{ab}\delta_{ab}$ is not so small, a simulation marker $v_i \simeq 0$ receives an intense drug force $-\gamma_{v^2}^{ab}v_i^2\Delta t$. Another problem of the C_v^{ab} operator at $v_i \sim 0$ is that the range of $v_i'^2$. Taking the derivative $dv_i'^2/dv_i$ of Eq. (A.8) with $\delta R = -1$, one finds that the minimum value of $v_i'^2$ occurs when

$$v_i = v_{ip} \equiv \frac{2v_a\sqrt{\frac{\alpha_{ab}\delta_{ab}}{3\sqrt{\pi}}}}{1 - \frac{8\alpha_{ab}\delta_{ab}}{3\sqrt{\pi}}}. \tag{A.10}$$

Though Eqs. (A.8) and (A.10) are valid only if $\alpha_{ab}\delta_{ab} \ll 1$, these approximated expressions suggest that the range of $v_i'^2$ is not bounded to $(0, +\infty)$, but $v_i'^2$ can even become negative around $v_i = v_{ip}$ for some cases, depending on the parameter $\alpha_{ab}\delta_{ab}$. Figures A.1(a-c) show the profiles of $x_{a1}^2 = v_i'^2/v_a^2$ as functions of $x_{a0}^2 = v_i^2/v_a^2$ which are calculated from Eq. (A.5) for several choises of $(\alpha_{ab}, \delta_{ab})$. It is found that the lower curve of x_{a1}^2, which correspond to the cases of $\delta R = -1$, becomes negative if $\alpha_{ab}\delta_{ab} >\sim 0.01$. Also, at $x_{a0}^2 \to 0$, it can be seen that x_{a1}^2 follows Eq. (A.9). In summary, the Monte Carlo impremention of C_{ab}^v by Eq. (A.5) is not valid around $x_a \simeq 0$ if $\alpha_{ab} \gg 1$ even if a small time step size $\delta_{ab} = \Delta t/\tau_{ab}$ is chosen. This imposes a more severe condition on the choise of Δt than that is required in the Lorentz operator. Since $\alpha_{ab} = v_a/v_b \sim \sqrt{m_b/m_a}$, this becomes a problem for a light species test-particle collisions with very heavy species. In the ion-ion collisions such as H-Fe and H-W in Sec. 4.1, α_{ab} is about 10 at most, and therefore this problem did not matter in practice. For electron-ion collisions, however, $\alpha_{ab} \sim 50$ and one should choose very small δ_{ab} to avoid this problem. The other way to avoid the problem is to adopt the

large-mass-ratio approximation, i. e., the light-to-heavy species test-particle operator is approximated only by the Lorentz pitch-angle scattering operator and therefore the energy transfer from a heavy to a light species is neglected. Sugama has shown that there is a way to consruct a linearized collision operator in the large-mass-ratio approximation which satisfies the momentum conservation and self-adjointness, though the energy conservation is not fully satisfied when $T_a \neq T_b$ [7].

References

[1] F. L. Hinton and R.D. Hazeltine, Rev. Mod. Phys. 48 (1976) 239.

[2] S. P. Hirshman and D. J. Sigmar, Nuclear Fusion 21 (1981) 1079.

[3] P. Helander, D. J. Sigmar, *Collisional Transport in Magnetized Plasmas*, Cambridge University Press, Cambridge, 2002.

[4] M. Shimada, D. J. Campbell, V. Mukhovatov et al., Nucl. Fusion 47 (2007) S1.

[5] F. L. Hinton, *Handbook of Plasma Physics* Vol. 1, Chapter 1.5, North-Holland Publishing Company, Amesterdam, (1983).

[6] H. Sugama and W. Horton, Phys. Plasmas 3 (1996) 304.

[7] H. Sugama, T.-H. Watanabe, and M. Nunami, Phys. Plasmas 16 (2009) 112503.

[8] S. Satake, R. Kanno, and H. Sugama, Plasma Fusion Res. 3 (2008) S1062.

[9] S. Matsuoka , S. Satake, R. Kanno, and H. Sugama, Phys. Plasmas 22 (2015) 072511.

[10] M. Nunami, M. Nakata, T.-H. Watanabe, and H. Sugama, Plasma Fusion Res. 10 (2015) 1403058.

[11] M. Nakata, M. Nunami, T.-H. Watanabe, and H. Sugama, Comp. Phys. Comm. 197 (2015) 61.

[12] K. Nanbu, Phys. Rev. E 55 (1997) 4642.

[13] A. H. Boozer and G. K.-Petravic, Phys. Fluids 24 (1981) 851.

[14] Z. Lin, W. M. Tang, and W. W. Lee, Phys. Plasmas 2 (1995) 2975.

[15] W. X. Wang, N. Nakajima, M. Okamoto, and S. Murakami, Plasma Phys. Control. Fusion 41 (1999) 1091.

[16] S. Brunner, E. Valeo, and J. A. Krommes, Phys. Plasmas 6 (1999) 4504.

[17] R. A. Kolesnikov, W. X. Wang, and F. L. Hinton, Journal of Comp. Phys. 229 (2010) 5564.

[18] S. Satake, Y. Idomura, H. Sugama, and T.-H. Watanabe, Comp. Phys. Comm. 181 (2010) 1069.

[19] G. Hu and J. A. Krommes, Phys. Plasmas 1 (1994) 863.

[20] S. Satake, M. Okamoto, N. Nakajima et al., Plasma Fusion Res. 1 (2006) 002.

[21] M. Honda, Japanese Journal of Appl. Phys. 52 (2013) 108002.

[22] M. Matsumoto and T. Nishimura, *Monte Carlo and Quasi-Monte Carlo Methods 1998*, pp 56-69, Springer (2000).

[23] S. Satake, M. Okamoto, N. Nakajima and H. Takamaru, *Lecture Notes in Computer Science* Vol. 4759, pp 344-357, Springer-Verlag, Berlin Heidelberg (2008).

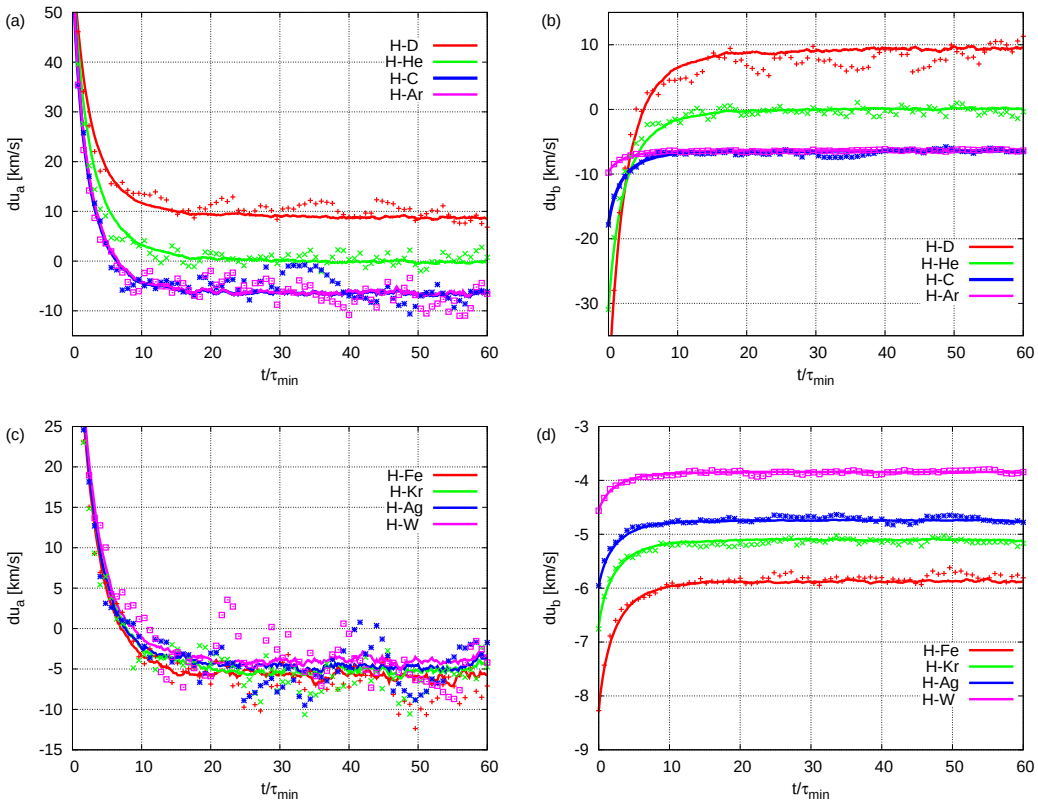

Figure 1: Time evolution of parallel mean flow δu of two ion species plasmas, a =H^+ and b = (D, T, $\cdots$, W)$^{2+}$. Figures (a) and (b) are the results of lighter b species, while (c) and (d) are heavier b species, respectively. Simulation results from the δf code with linearized collision operator are shown by solid curves and those from full-f PIC with Nanbu operator are plotted by points. Horizontal axis is time normalized by collision time τ_{min}, which is the minimum value of $\tau_{ij}(i, j = a \text{ or } b)$ in each case.

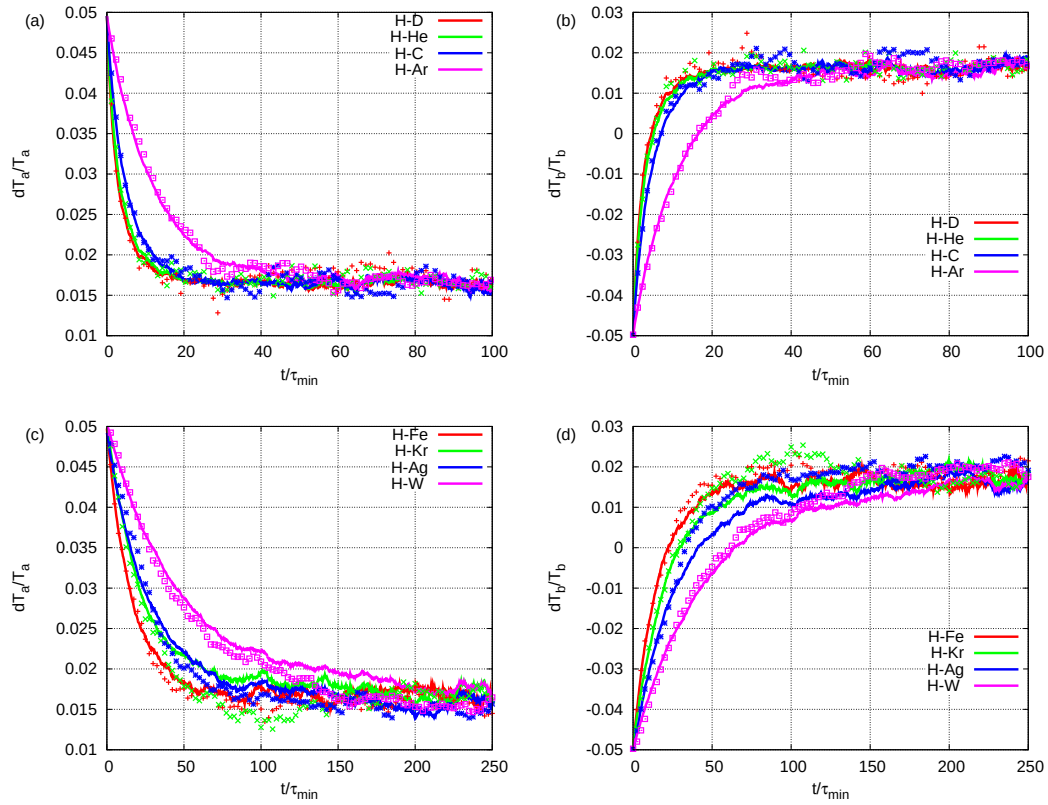

Figure 2: Time evolution of temperature perturbation $\delta T/T$ of two ion species plasmas. Simulation results from the δf code with linearized collision operator are shown by solid curves and those from full-f PIC with Nanbu operator are plotted by points.

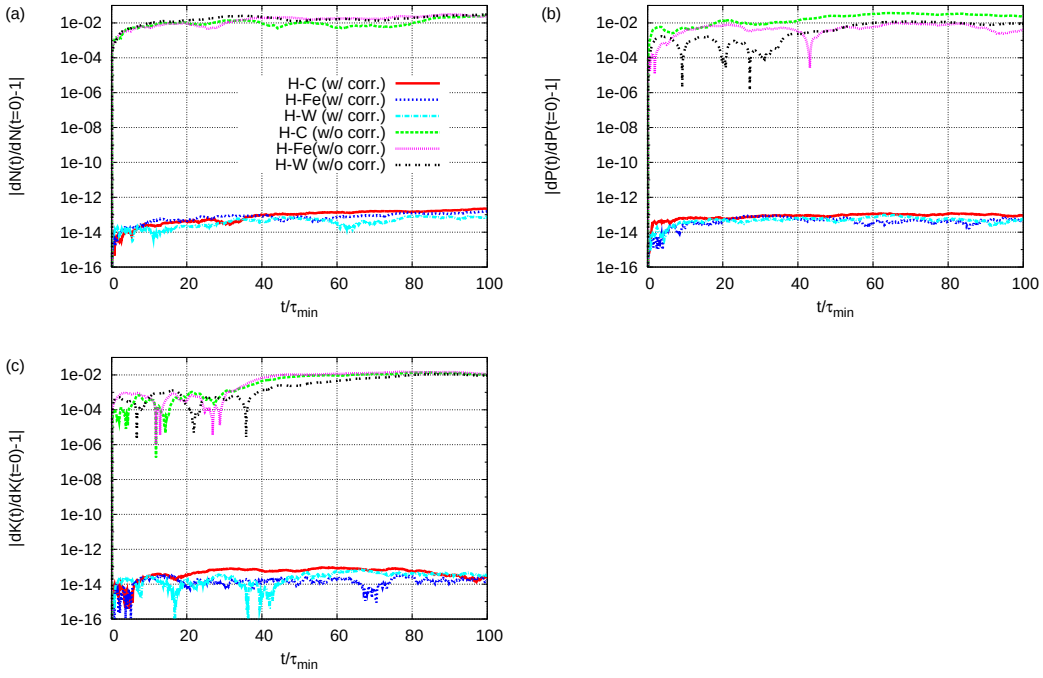

Figure 3: Relative error in the (a) total particle number δN, (b) parallel momentum δP, and (c) kinetic energy δK from their initial values in the case of a =H and b = (C, Fe, W) plasmas. "w/ corr." curves represent the calculations with the correction scheme in C_{ab}^F term to keep the conservation property, while "w/o corr." curves represent the calculations without correction, i. e., $(c_0, c_1, c_2) = (0, -1, -1)$ in Eq. (20).

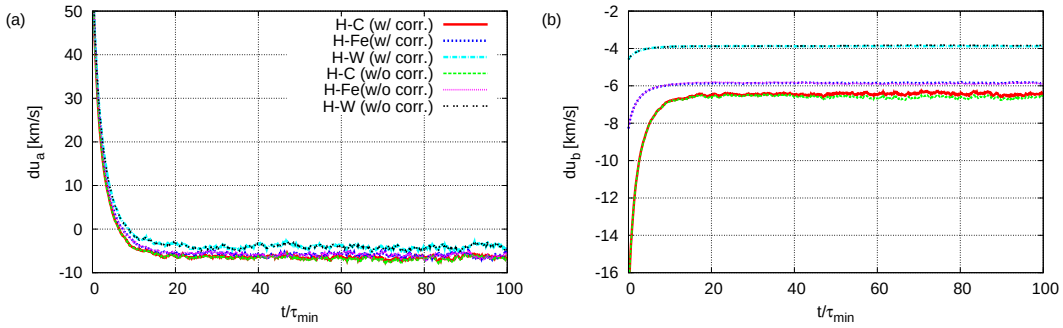

Figure 4: Time evolution of parallel mean flow, (a): δu_a and (b): δu_b in the case of a =H, b = (C, Fe, W) plasmas with or without the correction scheme in the C_{ab}^F term to keep the conservation property.

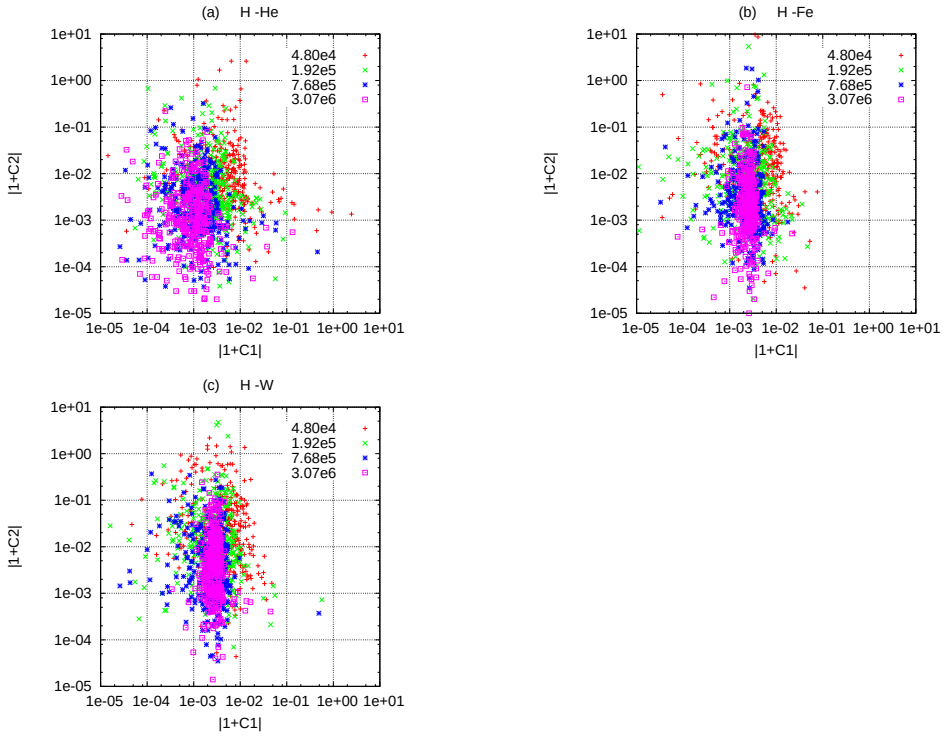

Figure 5: The distribution of the correction coefficients c_1 and c_2 in C^F_{ab} term in the case of a =H, b = (C, Fe, W) plasmas. Total number of simulation markers (written in the legend in the figures) are varied in these 4 cases. $|1 + c_{1,2}| \to 0$ is the ideal limit if the numerical error vanishes completely in the velocity integrals.

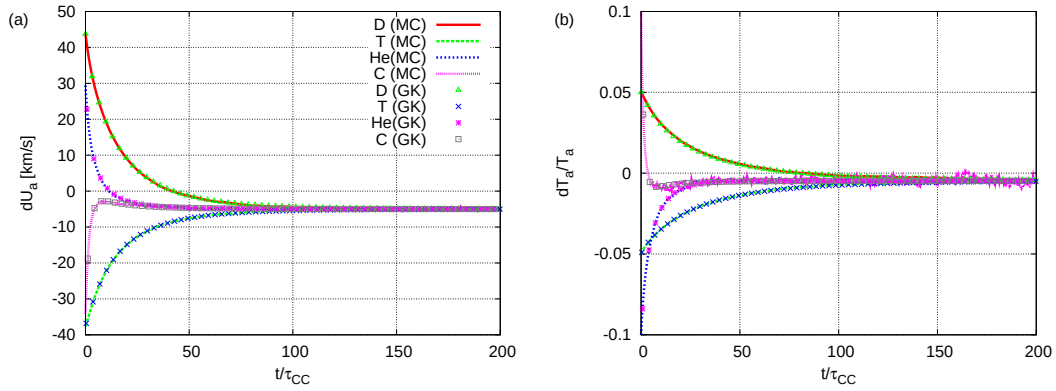

Figure 6: Time evolution of (a): mean flow δu and (b) : temperature perturbation $\delta T/T$ in the 4-species plasma. Simulation results from the δf Monte Carlo code (MC) are plotted by curves, and those from the continuum gyrokinetic δf code (GK) are plotted by points. Note that the MC simulation does not apply the weight averaging method discussed later in Section 4.2.

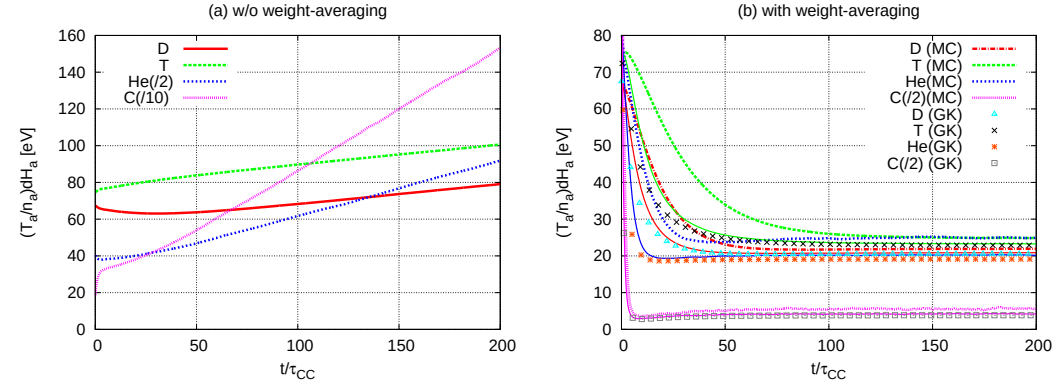

Figure 7: Time evolution of the quantities $(T_a/n_a)\delta H_a$ defined in Eq. (27) in the 4-species calculation. Fig 6(a) is the case without weight averaging, and 6(b) shows the cases with averaging, $f_W = 1$ (thick dotted lines) and $f_W = 5$ (thin solid lines). In Fig 6(b), the δH_a from the continuum gyrokinetic δf code (GK) are also plotted by points.

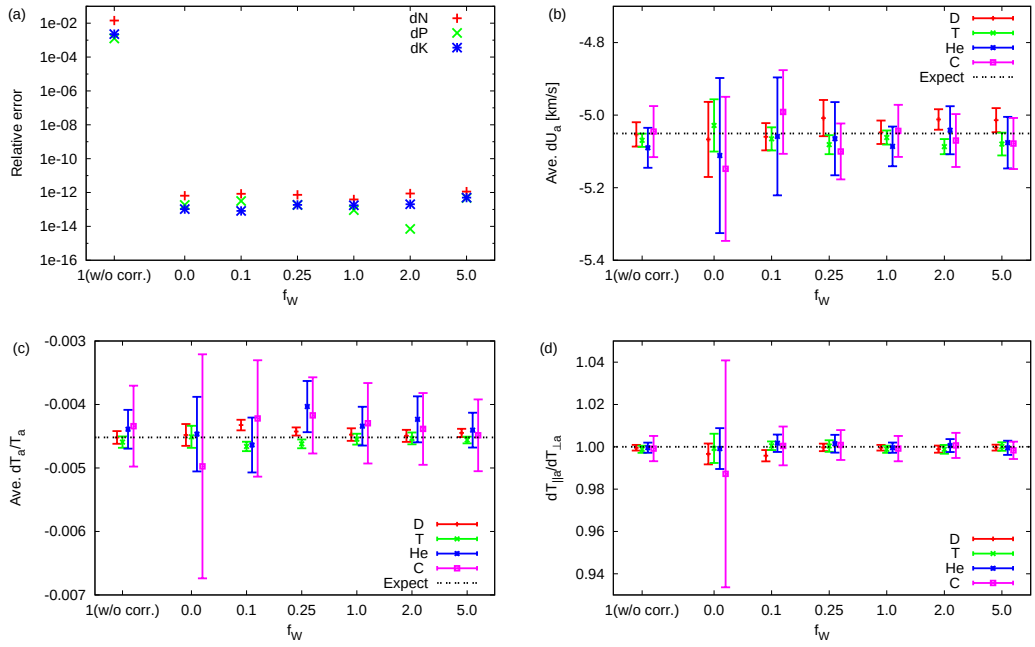

Figure 8: Dependence on the strength parameter of weight averaging method f_W on the time average of (a): relative error in the conserved quantities δN, δP and δK (the same as the quantities shown in Fig. 3), (b): mean flow δU_a, (c): temperature perturbation $\delta T_a/T_a$, and (d): temperature anisotropy $\delta T_{\parallel a}/\delta T_{\perp a}$, in the 4-species plasma. The averages and standard deviations of these quantities were evaluated from $t = 250$ to $300\tau_{CC}$. $f_W = 0$ means the no averaging, and $f_W = 5$ is the strongest averaging case. The leftmost points represent the $f_W = 1$ case without using the correction scheme in C^F_{ab} for the conservation property. Expectation values in Fig. 8(b) and (c) are estimated according to Eq. (26).

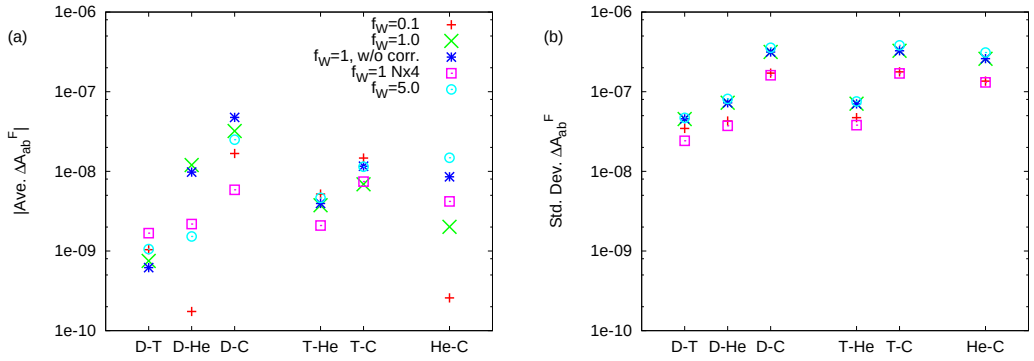

Figure 9: (a) Average and (b) standard deviation of ΔA_{ab}^F defined in Eq. (31) for the unlike-particle collisions in the 4-species simulation with varying the strength of weight averaging (f_W =0.1, 1, or 5). The correction method in C_{ab}^F were turned on in all the simulations except for the "w/o corr." case. The symbols of "$N \times 4$" represents the result using four times larger the number of simulation markers than the others. The average and standard deviation were evaluated by sampling ΔA_{ab}^F from the last $50\tau_{CC}$ part of each simulation (2×10^5 samples).

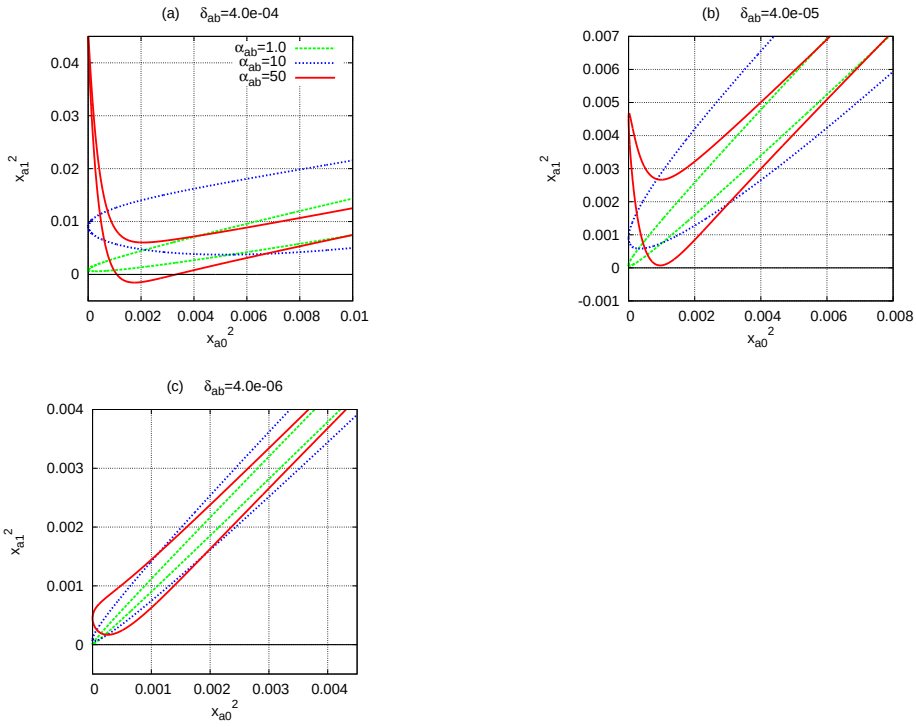

Figure A.1: Profiles of $x_{a1}^2 = v_i'^2/v_a^2$ as functions of $x_{a0}^2 = v_i^2/v_a^2$ which are calculated from the Monte Carlo test-particle operator C_v^{ab}, Eq. (A.5), for several choices of the parameters $(\alpha_{ab}, \delta_{ab})$. The upper and lower curves for each α_{ab} represent the values of x_{a1}^2 when the random number $\delta R = +1$ or -1, respectively. The region in which $x_{a1}^2 < 0$ for the $\alpha_{ab} = 50$ case in Fig. A.1(a) means the Monte Calro operator is incorrect there.